Journal of Environmental Chemical Engineering 6 (2018) 5221–5229

Contents lists available at ScienceDirect

Journal of Environmental Chemical Engineering

journal homepage: www.elsevier.com/locate/jece

Development of rice straw activated carbon and its utilizations

Hyungseok Nam[a,b,*], Woongchul Choi[c], Divine A. Genuino[a], Sergio C. Capareda[a]

[a] Bio-Energy Test and Analysis Laboratory (BETA Lab), Biological and Agricultural Engineering Department, Texas A&M University, College Station, TX 77843, USA
[b] Greenhouse Gas Laboratory, Korea Institute of Energy Research, Daejeon, 34129, Republic of Korea
[c] Material Science and Engineering Department, Texas A&M University, College Station, TX 77843, USA

ARTICLE INFO

Keywords:
Rice straw
Activated carbon
Nickel
Bio-oil upgrading
Pharmaceutical adsorption
Supercapacitor

ABSTRACT

Unrecycled wastes such as rice straw must be responsibly disposed to prevent environmental issues and it would be even better if it makes a profit. Pyrolysis as a thermal conversion process is one option to convert wastes into biochar, which can be used as a catalyst support for bio-oil catalytic upgrading, electrochemical material, and pollutant adsorbent after biochar activation. In the study, KOH chemical activation was applied to have high surface areas (1330 m^2/g). For the first application, the nickel impregnated on the activated carbon was used to upgrade the microalgae distilled bio-oil fraction. The upgraded bio-oil was deoxygenated by 42% and desulfurized by 86%. The H/C and O/C ratios of upgraded bio-oil showed close ratios of the petro-based fuels and HHV was obtained as about 42 MJ/kg. Most olefin and nitrile groups were cracked or converted into smaller carbon chains whereas the amount of paraffin and aromatic groups increased. Also, the activated carbon was evaluated as an electrochemical material, a supercapacitor, which showed both the properties of EDLC (electrical double layer capacitor) and pseudocapacitance. The highest specific capacitance was obtained at 93 F/g, which showed a modest specific capacitance. Last, the activated carbon was used as an adsorbent material to remove pharmaceutical pollutions and almost 95% of them were removed in a 24 h contact time.

1. Introduction

Waste management, pollution management and energy production are three important fields to be explored and put into practice as the world population increases, especially in industrialized countries. Unrecycled (or unrecyclable) wastes must be responsibly disposed to prevent environmental issues. Among the biomass wastes, rice as a representative biomass is a major agricultural product in China and India [1] and 727 million tons of wastes are globally produced [2]. Even though rice straw has many applications such as bedding, feed and compost, the production of rice straw exceeds its use every year. In addition, a large amount of rice straw in many underdeveloped countries left as is or burned in the field.

Most solid wastes including rice wastes can be converted into biochar and bio-oil through thermal conversion processes such as pyrolysis and hydrothermal liquefaction [3,4]. The potential applications of biochar has been investigated and it can be used for combustible energy material, a soil amendment, and activated carbon [5,6]. Especially, the value of activated carbon, defined as a porous carbon with BET (Brunauer-Emmett-Teller) areas between 5 to over 3000 m^2/g [7], can vary based on how the carbon is used, such as chemical purification absorbent, electrical battery supercapacitor, and catalysts support [8]. Among the carbon activation methods, the chemical activation using a KOH solution is known as an effective activation method due to its more micropores and higher micropore volume as compared to that over a physical activation method using steam or CO_2 [8,9].

The pyrolytic bio-oil, a major product from the thermochemical process, is considered as a source for a potential fuel substitute or additive. However, bio-oil are generally difficult to use directly as they are composed of a wide range of molecular weights and unwanted chemicals, which requires further processing to be able to meet ASTM standards. Current bio-oil upgrading studies are mostly based on catalytic hydrotreatment to reduce the oxygen content [10] under high temperature and pressure conditions. Noble metal catalysts such as palladium (Pd) and ruthenium (Ru) were used in bio-oil hydrotreatment to understand the effectiveness of bio-oil upgrading. Wildschut et al. [11] also used Pd/C catalyst for a pyrolytic bio-oil upgrading and showed a better bio-oil properties (lower oxygen content and a high product yield) compared to that with Pt/C catalyst. During hydrotreatment, a high pressure condition was considered as an important variable because it not only helps a reaction between hydrogen and bio-oil, but also decreases the coke formation of coke [12]. Even though many

* Corresponding author at: Bio-Energy Test and Analysis Laboratory (BETA Lab), Biological and Agricultural Engineering Department, Texas A&M University, College Station, TX 77843, USA.
E-mail address: namhs219@kier.re.kr (H. Nam).

https://doi.org/10.1016/j.jece.2018.07.045
Received 26 March 2018; Received in revised form 1 July 2018; Accepted 22 July 2018
Available online 27 July 2018
2213-3437/

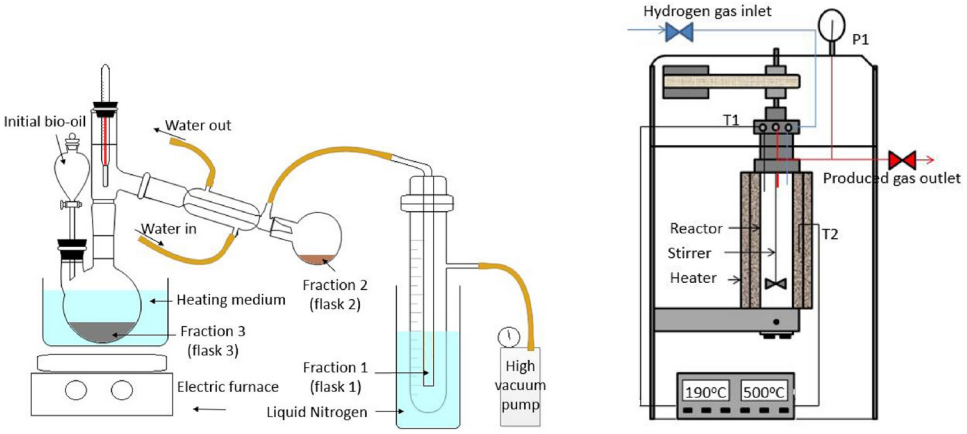

(a) Vacuum distillation setup [18] (b) Catalytic pressure reactor [19]

Fig. 1. Experimental set-up used for (a) distillation from Nam et al. [18] and (b) catalytic upgrading from Maguyon and Capareda [19].

studies found that a noble metal such as Pd and Pt improved the fuel quality, the unit price of palladium (Pd), $13,707/lb, is multiple times expensive than the unit price of nickel, $6.65/lb (reported by www.kitco.com on July 1st, 2018). One of major application of activated carbon can be a catalyst support due to its high porosity that can hold large amount of metal catalysts on the surface.

Other applications of activated carbon include supercapacitors (SC) as an electrochemical material application and adsorbent material for pollution removals. First, SC is based on both the electrostatic attraction and pseudocapacitance reactions (faradaic and redox reactions) so that it can reach a higher energy (the capacity to do work) density by maintaining the high power (how fast the energy is delivered) density as much as conventional capacitors. Even though the shape of the ideal voltammogram is rectangular, the typical activated carbon material shows the irregular rectangles due to its pseudocapacitance property. Adinaveen et al. [13] produced activated carbon using pyrolyzed rice straw with H_3PO_4 as an activating agent. A highest surface area of 376 m^2/g and a maximum capacitance of 112 F/g were obtained from activated carbon produced at 600 °C. Teo et al. [14] utilized rice husk wastes to make KOH activated carbon for a supercapacitor electrode. The highest surface area produced at 850 °C showed 2695 m^2/g of surface area and 147 F/g of specific capacitance. The common specific capacitance of activated carbon is known about 70–120 F/g in organic electrolytes [15]. Second, the activated carbon adsorbent has been approved for and widely used for removing color, odor and other pollutants mixed with water and air. Representative parameters used for a contaminant adsorption study include the pH of the solution, contact time, initial contaminant concentration, adsorbent dose and process temperature. The pH of an aqueous solution normally varies in an increase or a decrease in the negative charges on the adsorbent surface, which deals with the electrostatic force between the adsorbent and adsorbate ions. The lower the pH (acidized), the higher the protonation tendency of the adsorbent. Luna et al. [16] conducted the removal of Eriochrome Black T dye using RHAC (rice straw activated carbon) to find the optimum conditions based on initial concentration, adsorbent dose and pH. The highest removal of 95.9% was made. Mashayekh and Moussavi [17] used pomegranate wood activated carbon to remove acetaminophen pollution from water. The significant removal was made under the conditions of a pH of 2–8, a short contact time less than 5 min, and a low concentration of adsorbent achieving a maximum 233 mg/g adsorption capacity.

In this study,

1 The effect of temperature on chemical activation of rice straw (RS) bio-char was investigated to obtain an activated carbon with the highest surface area and micropores.
2 The nickel supported on activated carbon (Ni/AC) was used to upgrade vacuum distilled microalgae bio-oil for fuel substitutes or additives.
3 The effectiveness of produced activated carbon as supercapacitance material and water pollutant absorbent was evaluated.

2. Experimental

2.1. Materials

Bio-char (BC) for activated carbon synthesis was obtained from the pyrolysis process with rice straw and Ashe Juniper logs from Beaumont, Texas and Hill County, Texas, respectively. The pyrolysis condition for biochar production was set at 500 °C for 30 min using a batch type reactor as discussed in detail in a previous study [3]. Commercial activated carbon of mesh 20–40, nickel nitrate hexahydrate ($Ni(NO_3)_2$*$6H_2O$), KOH pellet, hydrochloric acid (HCl), H_2SO_4 used for electrolyte, and 5% Pd/C catalyst were purchased from Sigma Aldrich, USA. In addition, nafion solution (Fuel Cell Earth) for supercapacitor binder was obtained from MTI Corp, USA. Acetaminophen (Tylenol) and ibuprofen (Advil) were purchased from a local store (CVS). Microalgae pyrolytic bio-oil was produced to find the effectiveness of the metal supported on the activated carbon. A batch type pyrolysis reactor was utilized to pyrolyze microalgae (*Nannochloropsis oculata*) at 500 °C for a 30 min residence time. The produced pyrolytic bio-oil was then fractionated into the distillate fraction 1, 2, and 3 using a vacuum distillation setup as shown in Fig. 1(a) and the only fraction 2 was used for bio-oil upgrading in the current study. A further process condition on the bio-oil production is explained in detail from a previous study [10,18].

The rice straw bio-char (RSBC) was chemically activated using a KOH solution. The char, sieved with US Mesh 20 and 40 (85–425 μm), was impregnated in 8 M KOH solutions for 3 h at room temperature with a magnetic stirrer at 600 rpm. Then the sample was oven dried at 105 °C overnight. The oven dried sample was activated at temperatures of 550, 650, 750 and 850 °C for 30 min. under a nitrogen flow of 0.5 L/min. AC was washed with deionized water before a 0.1 M HCl solution was used for an hour-long acidic treatment to remove impurities. The deionized water was again used to wash the AC until the pH was close to 7.0. The neutralized AC was then finally dried in a 105 °C oven overnight. As 750 °C showed the highest surface area with rice straw activated carbon, the only temperature was selected to activate Ashe Juniper biochar for activation to evaluate AC as an electrochemical material.

The prepared AC and C (commercial activated carbon) supports were used for Ni impregnation. The carbon was soaked in the solution

of 0.05 g $Ni(NO_3)_2$/mL for 12 h at a 600 rpm and 40 °C. The amount of solution was determined based on the weight of the AC and C to make a 10% Ni loading on the activated carbon. The impregnated catalysts were then dried in a 105 °C oven overnight. The catalysts were identified as Ni/AC (10 wt.% Ni supported on the prepared activated carbon) and Ni/C (10 wt.% Ni supported on the commercial activated carbon). The developed activated carbon from the bio-char and commercial activated carbon are abbreviated as AC and C, respectively (eg. RSAC750: rice straw activated carbon activated at 750 °C, Ni/AC: nickel on activated carbon, and Ni/C: nickel on commercially purchased activated carbon).

2.2. Experimental setup and procedure of bio-oil upgrading

A distillation setup and a batch type pressure reactor as shown in Fig. 1 were utilized to distill the microalgae bio-oil and upgrade the pyrolytic bio-oil. Each run was made with 7 g of bio-oil with a 5 wt.% of prepared catalyst. Initially, hydrogen gas was used to flush the air from inside the reactor as much as possible. Then the reactor was pressurized with 4.1 MPa of hydrogen gas at a room temperature. Once the experiment was ready to run, the jacket furnace heated the reactor to 190 °C and held for 3 h at 400 rpm. After the reaction was done, the reactor was quenched to room temperature. Then the produced gas was first sampled for analysis before the pressure was completely released. Finally, the upgraded bio-oil was collected after filtering a Ni/AC catalyst using a pre-weighted class filter. Then the remaining catalyst and bio-oil in the reactor were washed out thoroughly using acetone. Both the class filter and washed bio-oil were dried in a 60 °C oven to completely remove the acetone solvent. The weight of the dried catalyst and washed bio-oil were identified as coke and tar, respectively, to complete the mass balance according to Eq. (1). Also, the deoxygenation and denitrogenation were obtained based on Eq. (2). The experiment of bio-oil upgrading was performed twice and averaged.

$$\text{Product yield (\%)} = \text{Mass of product (g)} / (\text{Initial bio-oil (g)} + \text{Consumed } H_2\text{ (g)}) \quad (1)$$

where mass of product: weight of each bio-oil, coke and tar product (g)

$$\text{DOD (\%)} = [\text{oxygen}_{\text{feed}}\ (\%) - \text{oxygen}_{\text{product}}\ (\%)] / \text{oxygen}_{\text{feed}}\ (\%) \times 100 \quad (2)$$

2.3. Electrochemical measurements

The activated carbon was evaluated as an electrochemical material. Initially, the supercapacitance black ink samples were prepared by mixing 7 mg of RSAC750, 160 μL of 5 wt.% Nafion solution (Fuel Cell Earth) in a solution of DI water (500 μL), and ethanol (170 μL). Then the prepared ink was well dispersed using a sonicator (FB-120, Fisher Scientific) for more than 1 h before it was loaded on a glassy carbon electrode of BASi. The ink on the electrode was oven dried at 40 °C for the cyclic voltammetry (CV) experiment. CV tests were carried out with a three-electrode system using a 604D CHI electrochemical station in a 0.5 M H_2SO_4 electrolyte. The three electrodes were composed of a working electrode with an AC sample, a Pt wire as a counter electrode, and an Ag/AgCl electrode in saturated KCl as a reference electrode. Nitrogen was continuously purged to the electrolyte. For a comparison purpose, a commercial activated carbon and Ash Junipers activated carbon were also prepared for electrochemical measurements.

2.4. Acetaminophen and ibuprofen adsorption

Acetaminophen and ibuprofen solutions of 10 mg/L were initially prepared using analytical grade ethanol solution and pharmaceutical powers of acetaminophen and ibuprofen. As the RSAC750 sample showed the highest surface area, this carbon was selected as an adsorbent and 0.05 g of AC was added into the 100 ml of pharmaceutical solution after adjusting the pH value to 4.0 using a 1.0 M H_2SO_4 solution. The adsorbance characteristics were determined using a UV–vis (Shimadzu). The calibration curve was constructed using an initial concentration from 2 to 10 mg/L for both the solutions of acetaminophen and ibuprofen. The 10 mg/L concentrate of both solutions with the activated carbon were agitated for 24 h before the last scans to understand the final concentration of chemicals.

2.5. Analytical methods

The size characterization of activated carbon was analyzed using a Quantachrome Instrument (autosorb-iQ model). First, the samples were degassed for 3 h at 300 °C. The adsorption and desorption isotherms were also measured at the relative pressures (0.0–1.0) of N_2 adsorption under a −196 °C chamber. A specific surface area (m^2/g), pore volume (m^3/g) and pore size distribution were determined based on a carbon equilibrium slit-pore model (NLDFT, non-local density functional theory). XRD (X-ray diffraction) patterns using a Bruker-AXS D8 VARIO were examined to understand the inorganic compounds. The Cu Kα radiation was set from $2\Theta = 20$ to 60° with a step size of 0.007°. The AC and nickel impregnated AC morphology were obtained by a Hittachi S-2400 SEM (Scanning electron microscope) and the elements were scanned using an EDS (energy dispersive x-ray spectroscopy). The EDS of the used catalyst was also done to check any elemental composition changes.

The pyrolytic bio-oil, distillated bio-oil and upgraded bio-oil were analyzed using the following analytical methods. A Vario MICRO Elemental analyzer was for determining carbon, hydrogen, nitrogen and sulfur contents in accordance with ASTM D5373. The oxygen content was determined by difference assuming there was no ash in the bio-oils. The HHV (higher heating value) was obtained using a Parr bomb calorimeter (ASTM D711). The ASTM E203 based a Karl-Fisher Titration setup was used to find the moisture content. A color titration indication method of ASTM D974 was used to find the TAN (total acid number). A GCMS (Shimadzu QP2010Plus), equipped with a 30 m × 0.25 mm × 0.25 μm thick, was used to determine the chemical compositions of the bio-oils using the same temperature ramping program used in a previous distillation study [18].

3. Results and discussion

3.1. Characteristics of the activated carbon

The N_2 adsorption-desorption isotherms of the RSACs and Ni/AC samples at −196 °C were done as shown in Fig. 2(a). According to the IUPAC guidelines and a reference [7], all the RSACs showed a combination of Type I (b) and Type II isotherms with Type H4 hysteresis (slit-shaped pores). Type 1 (b) indicates the existence of wide micropores, different from the narrow micropores of Type 1 (a), which can be understood from the round knee at a relative pressure (P/P_o) below 0.15 where the formation of monolayer finishes and the formation of multilayer begins. The narrow hysteresis loop due to interparticle capillary condensation indicates the presence of mesopores [7]. The capillary condensation caused the steeper slope with RSAC 650 °C compared to others, showing the existence of more mesopores above 35 Å width as found in Fig. 2(b). The pore size width of less than 20 Å is classified as micropores whereas the size between 20 and 500 Å is classified as mesopore. The activated carbon mostly contained micropores with some mesopores. The height of curvature at an initial relative pressure as illustrated in Fig. 2(a) was highly correlated to the pore size of less than 10 Å. The highest curvature was Ni/AC, followed by RSAC750, RSAC850, RSAC650, and RSAC550. Other than the width of less than 10 Å, the peak pore widths were found at 11.7 Å with Ni/AC, 10.6 Å with RSAC750, 12.9 Å with RSAC850, 13.3 Å with RSAC650, and 11.8 Å with RSAC550.

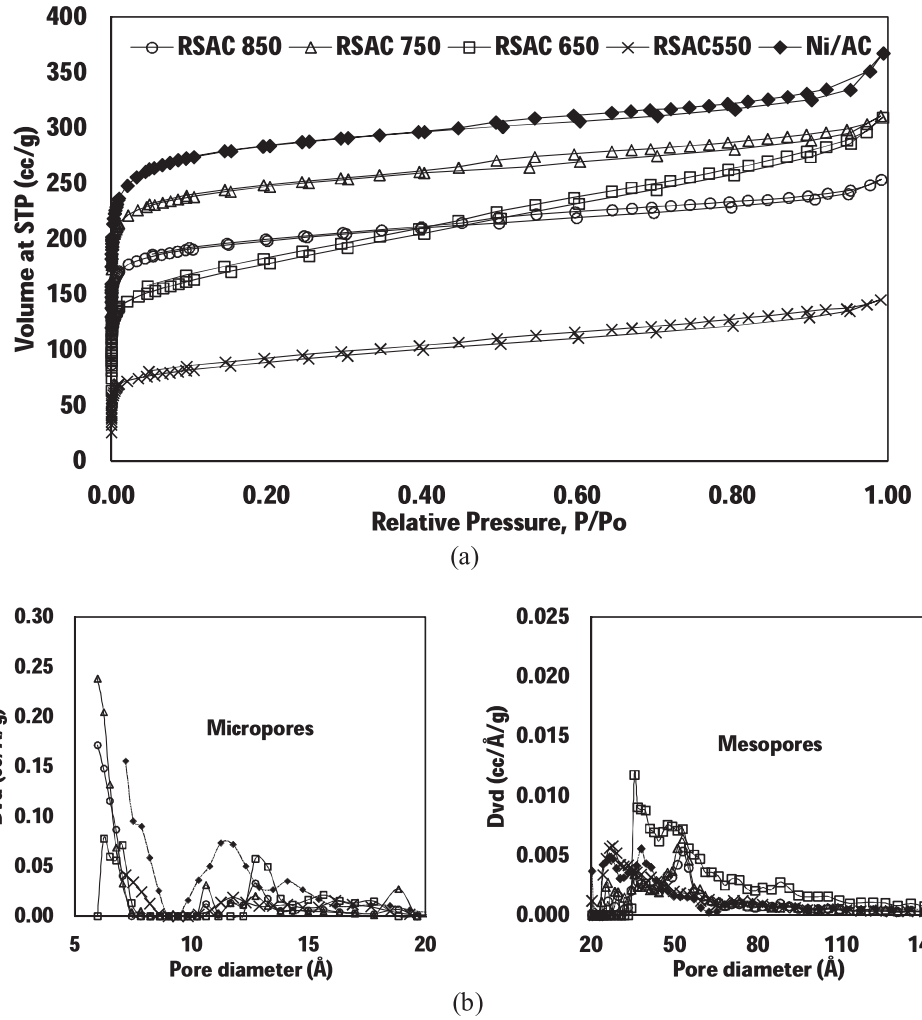

Fig. 2. Analysis of (a) adsorption-desorption isotherms and (b) pore size distribution of activated carbons.

Table 1
BET surface areas and pore volumes of activated carbons (RSAC stands for rice straw activated carbon, RHAC stands for rice husk activated carbon).

	Surface area (m^2/g)	Micropore surface area	Pore volume (cm^3/g)	Micropore pore volume
RS char	6.0 ± 0.2	N/A	N/A	N/A
RSAC 550	373.2 ± 3	309.0	0.200	0.146
RSAC 650	870.6 ± 21	783.2	0.445	0.271
RSAC 750	1330.5 ± 54	1304.5	0.522	0.508
RSAC 850	1076.9 ± 10	1039.8	0.375	0.306
Ni/AC 750	1102.6 ± 7	1082.4	0.489	0.422
RSAC [21]	1154	–	0.67	0.434
RHAC [22]	2652	0.531	0.878	–
RHAC [23]	752	–	0.64	0.38

The BET surface area and the pore volumes are shown in Table 1. RS biochar (rice straw biochar) was obtained from a previous pyrolysis study using a fixed bed reactor [3] and the solid mass product recovery was about 47.7%. The product yield of KOH activated carbon at 750 °C was obtained as 42% of initial biochar weight. The largest surface area (1330.5 m^2/g) of the activated carbon was produced at 750 °C whereas the smallest (373 m^2/g) was obtained at 550 °C. The surface area at the highest operating temperature at 850 °C showed smaller value (1076 m^2/g) than that at 750 °C as a result of the breakage of the micropore walls forming larger meso/macropores [14]. This also led to a decrease in pore volume from 0.522 cm^3/g for RSAC750 to 0.375 cm^3/g for RSAC850. The surface area and the pore volume wasn't always related each other when two of RSAC 650 and 850 were compared; a higher pore volume with RSAC 650 and a broader surface area with RSAC 850. This can be caused by the different proportion of meso and micropores. The more mesopores induced a broader volume whereas more micropores resulted in a higher surface area. The nickel impregnation on RSAC750 decreased both the surface area and pore volume, similar to the study by Zhang et al. [20] that the surface area and volume of metal impregnated AC decreased after nickel impregnation.

Ultimate analysis of raw biomass, bio-char and activated carbons was done to investigate the elemental compositions of carbon, hydrogen, nitrogen and sulfur as shown in Table 2. The carbon content in biochar increased to 45% after pyrolysis at 500 °C and the oxygen was significantly reduced to 6% due to the combination of decarboxylation,

Table 2
Ultimate analysis of activated carbon of rice straw on a dry basis.

wt.%	C	H	N	S	O[a]	Ash	H/C	O/C
Rice straw[b]	36.6	4.90	0.77	0.230	32.0	21.7	1.61	0.66
RS char[b]	45.1	2.13	1.40	0.235	6.2	45.0	0.57	0.10
RSAC 550	64.8	2.75	1.80	0.106	17.0	13.6	0.51	0.20
RSAC 650	65.4	2.06	1.71	0.088	14.9	15.9	0.38	0.17
RSAC 750	67.5	1.09	0.54	0.052	9.1	21.8	0.19	0.10
RSAC 850	67.1	1.16	0.76	0.068	8.5	22.4	0.21	0.10

[a] By difference.
[b] The elemental and ash data was referenced from the previous study [3].

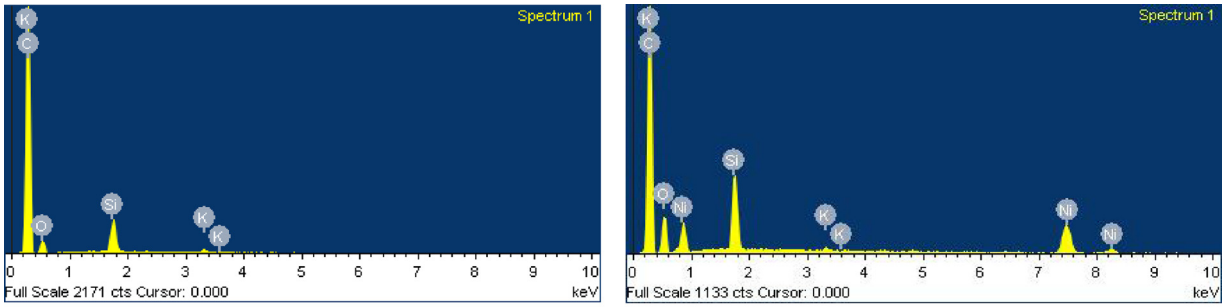

(a) (b)

Fig. 3. SEM and EDX of (a) activated carbon and (b) nickel impregnated carbon.

dehydration, and demethylation reactions. After the activation, the ash content was noticeably reduced at the lowest temperature of 550 °C. The hydrogen, nitrogen and oxygen contents at a higher temperature decreased due to a higher activation temperature, which led to a decrease in the H/C and O/C ratios at a higher temperature. Similar changes in elements of AC over KOH activation was reported previously; an increase in carbon and a decrease in hydrogen, nitrogen, and oxygen contents [24,25].

Fig. 3 shows EDX (energy dispersive X-rays) spectrums of RSAC (activated carbon) at 750 °C and Ni/AC, which scanned chemical compositions. The normalized nickel compositions on AC showed 9.1% after 6 scans, which is a similar value to the elemental data obtained from an ultimate analyzer shown in Table 2.

The XRD patterns of bio-char, activated carbons, and nickel impregnated carbons were analyzed and are presented in S. Fig. 1. As a previous study reported, the XRD patterns (1) of bio-char [3,5,26] included sylvite (KCl) at the angles at 2Θ = 28.3° and 40.4°, amorphous silica (cristobalite, SiO_2) at 2Θ = 22.5°, and quartz (SiO_2) at 2Θ = 26.6°. Also, broad peaks of 2Θ = 15° – 30° indicated randomly oriented aromatic layers in the amorphous carbon structure [25]. The broad peak at around 2Θ = 24° is attributed to an amorphous silica content in the untreated bio-char. The amorphous carbon patterns were reduced as a higher mole KOH solution and a higher activating temperature were applied as indicated at (2), (3) and (4). The complete removal of Ca and K related peaks by KOH washing was obtained from 8M KOH AC of (3) and (4). A further removal of the amorphous carbon peak of wide and weak was found from 8M KOH at 750 °C pattern, (4), indicating the presence of more ordered carbon structures. The XRD pattern confirmed the formation of more structured carbon along with increasing activation temperature conditions. The sharp peak on the pattern indicated a highly crystalline structure [13]. The patterns of (5) and (7) represented nickel impregnated on commercial activated carbon (6) and developed activated carbon (4) at 750 °C. Nickel peaks were determined at 44.5° on (111) plane and 51.8° on (200) plane, which was also detected in the same degree from a previous study [20]. This confirms the presence of nickel impregnated on the activated carbon.

3.2. Catalyst application for pyrolytic bio-oil upgrading

Upgrading of vacuum distilled microalgae bio-oil was performed using a developed Ni/AC and commercially available Pd/C under the operating conditions at 190 °C and 4.1 MPa with hydrogen gas. The condition used for a vacuum distillation was set at 120 °C and 90 Pa as reported in a previous study [10]. Table 3 shows the product yields of upgraded biofuel with two different catalysts of palladium (Pd) and nickel (Ni) impregnated on carbons. A Pd/C catalyst was chosen for bio-oil upgrading comparsion because it has been reported as the best catalysts for pyrolysis bio-oil hydrotreatment [10,11]. A higher product yield of 72% was found from Pd/C upgrading compared to a 63% yield with a Ni/AC catalyst. More gaseous products was produced with Ni/AC catalystas as compared to that with Pd/C, which indicates nickel catalyst helped better in cracking carbon chains. The amount of coke and tar was found at more or less 21% with both the catalysts and it was reported the amount of coke varied highly depending on the temperature and the residence time conditions [27].

The total acid number (TAN) and moisture content (MC) of bio-oil, distillated bio-oil and the upgraded bio-oils were measured as well as higher heating value (HHV) and element compositions as shown in Table 4. The TAN value shows the total acid chemicals in the bio-oil so that it directly indicates the concentration of acidic compounds that corrode metallic materials. A TAN of bio-oil (12.2 mgKOH/g) decreased to 0.1 mgKOH/g in the light fraction and increased to 21.5 mgKOH/g in the middle fraction after distillation [18]. TAN (21.5 mgKOH/g) of middle fraction (F2) after catalytic upgrading was significantly reduced to 5.7 mgKOH/g with Pd/C and 5.5 mgKOH/g with Ni/AC. An increase in a saturated hydrocarbon, converted from the unsaturated, mainly led to a decrease in TAN. By blending or further treatment, the TAN can be even reduced to meet the standards of petroleum based fuels. MC indicates the amount of water included in the fraction. An initial MC of 8.2% was greatly reduced in the distillation fractions (0.5–1.7%) whereas the MC of upgraded fractions (0.5–0.7%) was barely reduced from the vacuum distillated fractions (F2). The HHV of upgraded fuels from F2 (41.1 MJ/kg) was merely increased to 41.7 MJ/kg for Pd/C and 41.4 MJ/kg for Ni/AC. However, a higher HHV of distillates and upgrades was determined compared to HHVs of the direct microalgae bio-oil upgrading (37.5–39.6 MJ/kg) with a zeolite catalyst [28]. A hydrothermal catalytic study of pretreated microalgae oil by Bai et al. [29] reported that the upgraded bio-oil with Pd/C at 400 °C was 42.6 MJ/kg. The physical properties of MC and HHV of distillates and upgrades were close to the crude oil and biodiesel standards. The carbon and hydrogen content of bio-oil increased by 6% and 14% of upgraded bio-oil, respectively whereas the sulfur and oxygen contents decreased by 86% and 42%. Over the catalytic upgrading, many unsaturated hydrocarbons were saturated. The significant hydrodeoxygenation and hydrodesulfurization reactions through the catalytic

Table 3
Percentile yields of products after hydrotreatment.

	Temp. – Pressure	Yield	Coke	Tar	Loss + Gas
F2–5%Pd/C	190 °C – 4.1 MPa	72 ± 1.5%	7 ± 0.5%	13 ± 0.8%	7%
F2–10%Ni/AC	190 °C – 4.1 MPa	63 ± 3.2%	6 ± 0.2%	16 ± 0.4%	15%

Table 4
Physical and elemental properties of bio-oil, distillates and upgrades compared to the petroleum based fuels (V_F1: vacuum distilled fraction 1).

	TAN (mgKOH/g)	MC (%)	HHV (MJ/kg)	C	H	N	S	O[a]
Bio-oil [18]	12.2	8.2	38.6	72.2	9.7	6.0	0.22	11.9
V_F1 [18]	0.10	1.7	40.5	66.3	9.4	4.1	0.20	19.9
V_F2 [18]	21.50	0.50	41.1	74.1	10.4	5.2	0.17	10.1
5% Pd/C of F2	5.73 ± 0.01	0.69	41.7 ± 0.1	76.6 ± 0.7	11.12 ± 0.2	5.3 ± 0.1	0.03 ± 0.0	6.93
10% Ni/AC of F2	5.46 ± 0.02	0.48	41.4 ± 0.0	76.6 ± 1.2	11.05 ± 0.1	5.2 ± 0.1	0.05 ± 0.0	7.05
Crude oil [21]	–	< 0.5	41 ~ 43	83-87	14-10	0.1-2	0.05-6	0.05-1.5
FAME [26]	< 0.5[b]	< 0.05[b]	39	76.2	12.6	–	–	11.2
Gasoline [27]	–	–	43 ~ 47	85-88	15-12	–	–	–

[a] By difference.
[b] Biodiesel standard – ASTM D6751.

hydrotreatment improved the fuel properties to be even close to petroleum based fuels. However, the nitrogen (5–6%) and oxygen (about 7%) contents still need a further treatment to be used directly in engines. By considering the comparable physical and elemental properties of upgraded bio-oil with nickel catalyst, it can be concluded that Pd/C performes better than Ni/AC. However, an important advantage of nickel (over 2000 times) is a cheaper cost, which can economically replace the expensive noble metal catalyst such as Pd.

For a better understanding of the upgraded elemental data, a Van Krevelen plot was used as shown in Fig. 4. H/C and O/C ratios of bio-oil were 1.61 and 0.12 and changed to H/C (1.68) and O/C (0.05) after distillation toward the direction of a decarboxylation reaction. Then the hydrogen enrichment and oxygen removals after the hydrotreating step upgraded the elemental ratios (H/C: 1.73–1.74 and O/C: 0.034 – 0.035) even closer to the ratios of petroleum based fuels. Previous upgrading studies showed the similar ranges of ratios. Bai et al. [29] reported H/C (1.64) and O/C (0.027) with Pd/C catalytic upgrading of microalgae bio-oil at 400 °C. Maguyon [28] showed H/C (1.55) and O/C (0.058) from zeolite catalytic upgrading with microalgae bio-oil at 250 °C.

The upgraded microalgae bio-oil chemical compounds were analyzed to understand the chemical transitions using GCMS. The compounds were sorted into several functional chemical groups of saturated hydrocarbons (paraffin and naphthene), unsaturated hydrocarbons (olefin and aromatic), N-containing (aromatic N. and nitrile), O-containing (ketone and other oxygenates), and others. For a better comparison, chemical compositions of bio-oil and vacuum fractionates were also categorized as shown in Fig. 5. Significant chemical transitions were made from unsaturated hydrocarbons to saturated hydrocarbons after the distillation and hydrotreatment of raw bio-oil. The relative percent of paraffin and olefin after distillation of raw bio-oil increased, and that of the ketone and nitrile decreased. An increase in saturated hydrocarbons and a decrease in ketone after distillation resulted in a better stabilized biofuel whereas the unsaturated hydrocarbon (olefin) was still high. A commercial 5% Pd/C and a developed 10% Ni/AC catalyst were used for the catalytic upgrading of distillated bio-oil (F2). The same tendency of chemical group transitions were recognized (an increase in saturated hydrocarbons and aromatics with a decrease in olefin and nitrogen/oxygen containing compounds). However, the degree of chemical group transitions were different depending on each catalyst (Pd/C and Ni/AC). A higher amount of saturated hydrocarbons with a Pd/C catalyst were obtained compared to the amount with a Ni/AC catalyst whereas a lower olefin and nitrile with Pd/C catalyst was obtained. The four most abundant chemicals from catalyst upgrading were undecane ($C_{11}H_{24}$), dodecane ($C_{12}H_{26}$), tridecane ($C_{13}H_{28}$), and hexadecane ($C_{16}H_{34}$), which comprised 54.2–56.5%.

The four major chemical groups of paraffin, olefin, total aromatics and nitrile were further analyzed based on carbon numbers as indicated in Fig. 6. The carbon ranges were decided based on the aviation fuel (C_8 – C_{16}), which can be separated with the distillation temperature of lower boiling point (126 °C) and upper boiling point (287 °C) [30]. The paraffin group, as indicated previously, showed the most amounts in a range of C_8–C_{16} that the paraffin distillate (47%) increased to 65% with Ni/AC and 73% with Pd/C. On the other hand, the olefin distillate (21%) in the C_8–C_{16} range decreased to 11% with Ni/AC and 7% with Pd/C. The unsaturated hydrocarbon of olefin was converted into saturated hydrocarbons through a hydrogenation reaction with an H_2 [31]. Similar to an increase in paraffin, the aromatics within a range of C_8–C_{16} increased almost twice the original percent over hydrotreatment with both catalysts. The upgrade with Ni/AC catalyst was prone to crack hydrocarbons as more of < C_8 aromatics were produced. The combination reactions of cracking, methylation, alkylation and dealkylation incurred the changes of chemical compositions over catalytic conversions [32]. A better removal of the nitrile group with Pd/C was made over all the different carbon ranges compared to the removal with Ni/AC.

The used catalysts for the hydrotreatment of bio-oil were investigated. The nitrogen and sulfur of both the catalysts were substantially increased. Especially, an increase in sulfur content indicates the removal of sulfur from bio-oil as shown in Table 5. Approximately 2% of the sulfur of bio-oil was decreased to 0.04% of upgraded bio-oil whereas the sulfur contents of the used catalyst increased from 0.05% to 2.21% for Ni/AC and 0.07% to 0.60% for Pd/C.

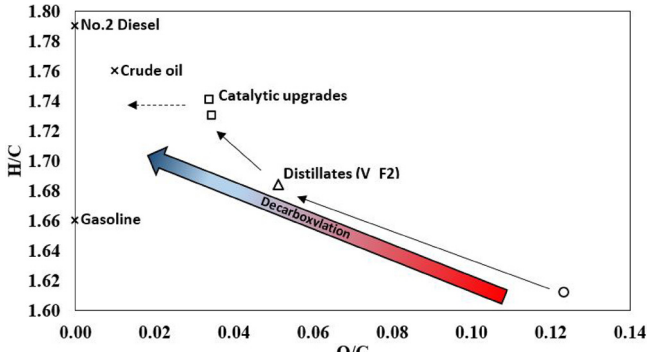

Fig. 4. Van Krevelen diagram of bio-oil, distillate, upgrades and petro-fuels.

3.3. Electrochemical material application as a supercapacitor

The electrochemical tests of the produced activated carbon were conducted to evaluate their performance as a supercapacitor. The performance of Ashe Juniper and rice straw activated carbon was compared to that of commercially available activated carbon. Fig. 7(a–c) indicates a specific capacitance (F/g) of three different biomass activated carbons at different sweep rates (10, 50, and 100 mV/s). Fig. 7(d) represents cyclic voltammograms of three samples at 10 mV/s for direct comparison purposes. A general trend in specific capacitance at an increasing sweep rate decreased from 42 to 30 F/g for a commercial carbon, 35 to 22 F/g for AJAC, and 93 to 56 F/g for RSAC because of ion diffusion and adsorption arrival delays inside the smallest pores. This phenomena is often observed in activated carbons [15]. At the slowest

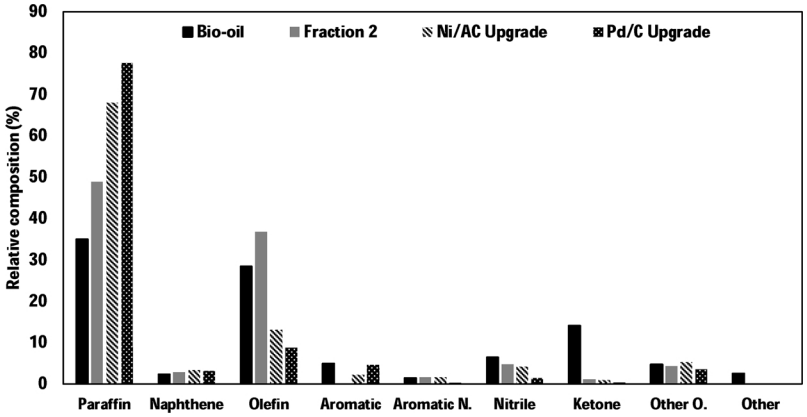

Fig. 5. Chemical groups of upgraded bio-fuel analyzed by GC–MS (Bio-oil and fraction 2 are imported from Nam et al. [18]).

sweep rate of 10 mV/s, the closest rectangular shape of a CV was obtained even though it was not symmetrical, indicating a substantial pseudocapacitance contribution to all of the carbons. The AJAC sample showed the worst symmetrical shape with peaks, which was associated with unbalanced reduction and oxidation (redox) reactions. On the other hand, the commercial carbon with the least oxygen containing functional groups among other samples showed the fewest redox reactions. The pseudocapacitance peaks had almost disappeared at the sweep rate of 100 mV/s with a commercial carbon.

A lower surface area of AJAC of 480 m^2/g and commercial carbon of 680 m^2/g contributed to a lower slope at the 0–0.2 V region as compared to that of RSAC, which also led to a smaller ion adsorption capacity. Even though the strongest EDLC electrode was found from a commercial carbon, the highest specific capacitance was found from RSAC with 93 F/g at 10 mV/s as indicated in Fig. 7(d). The obtained capacitance of RSAC was comparable to the commercially available supercapacitors of 70–120 F/g. ACM8 (activated carbon of green monoliths) in 1 M H_2SO_4 showed 80 F/g at 1 V and 1 mV/s [33]. Activated carbon of cellulose and wood in 1 M $TEABF_4$ (tetraethylammonium tetrafluoroborate salt) in acetonitrile, respectively, represented 140 F/g and 236 F/g at 2 V and 1 mV/s [15].

3.4. Adsorption of acetaminophen and ibuprofen

Table 6 shows the percent of acetaminophen and ibuprofen removal from the initial concentration. After 24 h of agitation of the pharmaceutical solution and activated carbon, the acetaminophen and ibuprofen were reduced by 95.0% and 95.3%, respectively, which was similar to the percent of removal reported by other studies; 95.9% of Eriochrome Black T dye using rice straw activated carbon by Luna et al.

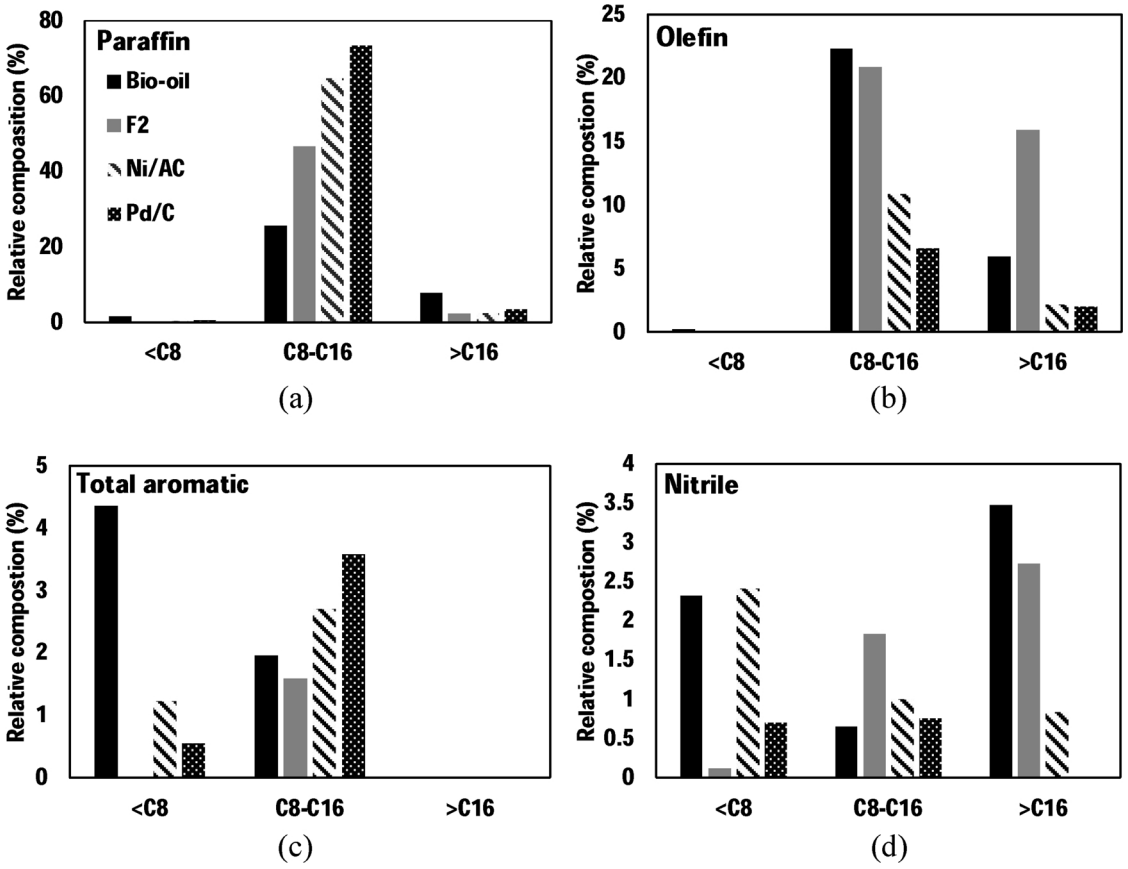

Fig. 6. Carbon number distributions of distilled and upgraded bio-oil based on the chemical groups.

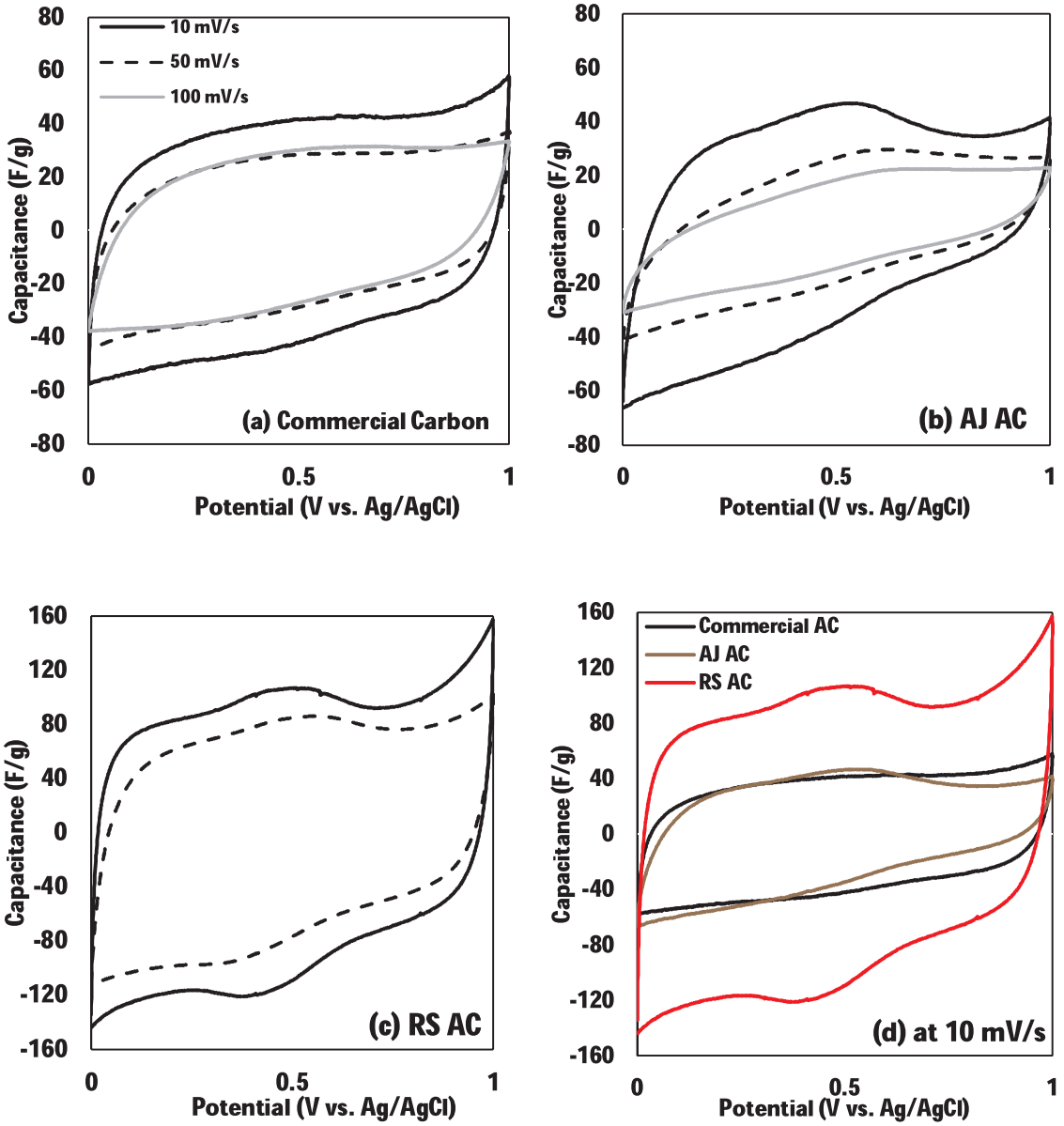

Fig. 7. Cyclic voltammograms of (a) commercial carbon, (b) Ashe Juniper activated carbon, (c) rice straw activated carbon, and (d) comparison voltammograms of three activated carbons at 10 mV/S.

Table 5
Elemental data for catalysts used after bio-oil upgrading.

VD F2 upgrading	C	H	N	S
RSAC 750	67.5	1.09	0.54	0.052
Used 10%Ni/AC	66.1	3.36	2.39	2.210
5%Pd/C	73.5	1.47	0.19	0.071
Used Pd/C	82.2	2.28	1.53	0.600

Table 6
Adsorptive removal of acetaminophen and ibuprofen solution using rice straw activated carbon at 750 °C.

Compounds	Initial conc.	Final conc.	% Removal
Acetaminophen	10.0 mg/L	0.50 mg/L	95.0%
Ibuprofen	10.0 mg/L	0.47 mg/L	95.3%

[16] and 99% of acetaminophen contaminant using pomegranate wood activated carbon by Mashayekh-Salehi and Moussavi [17]. The adsorption test was conducted under pH ranges from 2 to 12. The removal percent declined from 83 to 70% when the pH was decreased from 10 to 12 due to no electrostatic attraction occurrence at a higher pH. It was also determined by Liu et al. [34] that the removal percent of acetaminophen was almost constant (91–92%) under a pH from 2 to 9, while a pH above acetaminophen pK_a of 9.38 led to a significant removal rate of 70%. This was expected due to the electrostatic repulsion between the negatively charged activated carbon and anionic solution. In the case of ibuprofen, a pH $<$ 4 resulted in over 90% removal while a pH $>$ 4 led to a significant decrease due to electrostatic repulsion as reported by Mestre el al. [35]. This results indicated that the pH has to meet the acid-base property of the contaminant.

4. Conclusions

Bio-char, one of the major products from the pyrolysis, was utilized and upgraded to activated carbon. A KOH chemical activation was applied at different activation temperatures to find an optimum condition for the largest surface area and micropores. Then the

performance of activated carbon was evaluated as an adsorption material, a capacitance material, and a metal catalyst support for catalytic bio-oil upgrading. The largest surface area and micropores were found at the activation temperature of 750 °C (1330 m^2/g). The nickel impregnated on the activated carbon also successfully improved the vacuum distilled microalgae bio-oil by 42% deoxygenation and 86% desulfurization. The upgraded bio-oil product was recovered with a 63–72% yield. The H/C and O/C ratios of upgraded bio-oil from raw bio-oil was close to the petroleum based fuels. The paraffin and aromatic contents increased after upgrading whereas the olefin and nitrile compounds decreased and cracked to form smaller carbon chains. The activated carbon as a supercapacitor showed both EDLC (electrical double layer capacitor) and pseudocapacitance natures. The highest specific capacitance was obtained from RSAC at 93 F/g, followed by commercial carbon at 42 F/g and AJAC at 35 F/g, which showed a modest specific capacitance. Up to 95% of the acetaminophen and ibuprofen pollutants in an aqueous solution was removed using activated carbon after a 24 h contact time.

Acknowledgments

The authors acknowledge the facilities, and the scientific and financial assistance of the Bio Energy Testing and Analysis Laboratory (BETA lab) and AgriLife Research at Texas A&M University, USA. The work was also supported by the dissertation fellowship from OGAPS (Office of Graduate and Professional Studies) and undergraduate research scholarship from Honors & Undergraduate Research, Texas A&M University, USA. We gratefully thank Su-In Yi for his help on the XRD analysis.

Appendix A. Supplementary data

Supplementary material related to this article can be found, in the online version, at doi:https://doi.org/10.1016/j.jece.2018.07.045.

References

[1] FAOSTAT, Data From Food and Agriculture Organization of the United Nations, 2017, (2014).
[2] R. Bakker, H.W. Elbersen, R.P. Poppens, J.P. Lesschen, Rice Straw and Wheat Straw: Potential Feedstocks for the Biobased Economy, NL Energy and Climate Change, Utrecht, The Netherlands, 2013.
[3] H. Nam, S.C. Capareda, N. Ashwath, J. Kongkasawan, Experimental investigation of pyrolysis of rice straw using bench-scale auger, batch and fluidized bed reactors, Energy 93 (Part 2) (2015) 2384–2394.
[4] R. Shakya, S. Adhikari, R. Mahadevan, S.R. Shanmugam, H. Nam, E.B. Hassan, et al., Influence of biochemical composition during hydrothermal liquefaction of algae on product yields and fuel properties, Bioresour. Technol. 243 (2017) 1112–1120.
[5] W. Wu, M. Yang, Q. Feng, K. McGrouther, H. Wang, H. Lu, et al., Chemical characterization of rice straw-derived biochar for soil amendment, Biomass Bioenergy 47 (2012) 268–276.
[6] R. Sitthikhankaew, D. Chadwick, S. Assabumrungrat, N. Laosiripojana, Effect of KI and KOH impregnations over activated carbon on H2S adsorption performance at low and high temperatures, Sep. Sci. Technol. 49 (2014) 354–366.
[7] J. Rouquerol, F. Rouquerol, P. Llewellyn, G. Maurin, K.S. Sing, Adsorption by Powders and Porous Solids: Principles, Methodology and Applications, Academic press, Oxford, UK, Oxford, UK, 2013.
[8] J. Wang, S. Kaskel, KOH activation of carbon-based materials for energy storage, J. Mater. Chem. 22 (2012) 23710–23725.
[9] T. Otowa, R. Tanibata, M. Itoh, Production and adsorption characteristics of MAXSORB: high-surface-area active carbon, Gas Sep. Purif. 7 (1993) 241–245.
[10] H. Nam, C. Kim, S.C. Capareda, S. Adhikari, Catalytic upgrading of fractionated microalgae bio-oil (Nannochloropsis oculata) using a noble metal (Pd/C) catalyst, Algal Res. 24 (Part A) (2017) 188–198.
[11] J. Wildschut, F.H. Mahfud, R.H. Venderbosch, H.J. Heeres, Hydrotreatment of fast pyrolysis oil using heterogeneous noble-metal catalysts, Ind. Eng. Chem. Res. 48 (2009) 10324–10334.
[12] P.M. Mortensen, J. Grunwaldt, P.A. Jensen, K. Knudsen, A.D. Jensen, A review of catalytic upgrading of bio-oil to engine fuels, Appl. Catal. A Gen. 407 (2011) 1–19.
[13] T. Adinaveen, L.J. Kennedy, J.J. Vijaya, G. Sekaran, Surface and porous characterization of activated carbon prepared from pyrolysis of biomass (rice straw) by two-stage procedure and its applications in supercapacitor electrodes, J. Mater. Cycles Waste Manag. 17 (2015) 736–747.
[14] E.Y.L. Teo, L. Muniandy, E. Ng, F. Adam, A.R. Mohamed, R. Jose, et al., High surface area activated carbon from rice husk as a high performance supercapacitor electrode, Electrochim. Acta 192 (2016) 110–119.
[15] L. Wei, M. Sevilla, A.B. Fuertes, R. Mokaya, G. Yushin, Hydrothermal carbonization of abundant renewable natural organic chemicals for high-performance supercapacitor electrodes, Laser Phys. Rev. 1 (2011) 356–361.
[16] Mark de Luna, G. Daniel, E.D. Flores, D.A.D. Genuino, C.M. Futalan, M. Wan, Adsorption of Eriochrome Black T (EBT) dye using activated carbon prepared from waste rice hulls—optimization, isotherm and kinetic studies, J. Taiwan Inst. Chem. Eng. 44 (2013) 646–653.
[17] A. Mashayekh-Salehi, G. Moussavi, Removal of acetaminophen from the contaminated water using adsorption onto carbon activated with NH4Cl, Desalin. Water Treat. (2015) 1–13.
[18] H. Nam, J. Choi, S.C. Capareda, Comparative study of vacuum and fractional distillation using pyrolytic microalgae (Nannochloropsis oculata) bio-oil, Algal Res. 17 (2016) 87–96.
[19] M.C.C. Maguyon, S.C. Capareda, Evaluating the effects of temperature on pressurized pyrolysis of *Nannochloropsis oculata* based on products yields and characteristics, Energy Convers. Manage. 76 (2013) 764–773.
[20] J. Zhang, K. Yanagisawa, S. Yao, H. Wong, Y. Qiu, H. Zheng, Large-scale controllable preparation and performance of hierarchical nickel microstructures by a seed-mediated solution hydrogen reduction route, J. Mater. Chem. A 3 (2015) 7877–7887.
[21] W. Cao, Z. Dang, X. Zhou, X. Yi, P. Wu, N. Zhu, et al., Removal of sulphate from aqueous solution using modified rice straw: preparation, characterization and adsorption performance, Carbohydr. Polym. 85 (2011) 571–577.
[22] H. Nam, S. Wang, H. Jeong, TMA and H2S gas removals using metal loaded on rice husk activated carbon for indoor air purification, Fuel 213 (2018) 186–194.
[23] K.Y. Foo, B.H. Hameed, Utilization of rice husks as a feedstock for preparation of activated carbon by microwave induced KOH and K2CO3 activation, Bioresour. Technol. 102 (2011) 9814–9817.
[24] B. Xing, H. Guo, L. Chen, Z. Chen, C. Zhang, G. Huang, et al., Lignite-derived high surface area mesoporous activated carbons for electrochemical capacitors, Fuel Process Technol. 138 (2015) 734–742.
[25] J.T. Yu, A.M. Dehkhoda, N. Ellis, Development of biochar-based catalyst for transesterification of canola oil, Energy Fuels 25 (2010) 337–344.
[26] N. Prakongkep, R.J. Gilkes, W. Wiriyakitnateekul, A. Duangchan, T. Darunsontaya, The effects of pyrolysis conditions on the chemical and physical properties of Rice husk biochar, Int. J. Mater. Sci. (2013).
[27] S. Vitolo, M. Seggiani, P. Frediani, G. Ambrosini, L. Politi, Catalytic upgrading of pyrolytic oils to fuel over different zeolites, Fuel 78 (1999) 1147–1159.
[28] M. Maguyon, Technical Feasibility Study on Biofuels Production From Pyrolysis of *Nannochloropsis oculata* and Algal Bio-oil Upgrading, (2013).
[29] X. Bai, P. Duan, Y. Xu, A. Zhang, P.E. Savage, Hydrothermal catalytic processing of pretreated algal oil: a catalyst screening study, Fuel 120 (2014) 141–149.
[30] J.G. Speight, Handbook of Petroleum Product Analysis in Chapter 6 Page 105, John Wiley & Sons, 2015.
[31] D.R. Vardon, B.K. Sharma, H. Jaramillo, D. Kim, J.K. Choe, P.N. Ciesielski, et al., Hydrothermal catalytic processing of saturated and unsaturated fatty acids to hydrocarbons with glycerol for in situ hydrogen production, Green Chem. 16 (2014) 1507–1520.
[32] S. Ilias, R. Khare, A. Malek, A. Bhan, A descriptor for the relative propagation of the aromatic-and olefin-based cycles in methanol-to-hydrocarbons conversion on H-ZSM-5, J. Catal. 303 (2013) 135–140.
[33] N. Basri, B. Dolah, Physical and electrochemical properties of supercapacitor electrodes derived from carbon nanotube and biomass carbon, Int. J. Electrochem. Sci. 8 (2013) 257–273.
[34] H. Liu, W. Ning, P. Cheng, J. Zhang, Y. Wang, C. Zhang, Evaluation of animal hairs-based activated carbon for sorption of norfloxacin and acetaminophen by comparing with cattail fiber-based activated carbon, J. Anal. Appl. Pyrolysis 101 (2013) 156–165.
[35] A.S. Mestre, J. Pires, J.M.F. Nogueira, A.P. Carvalho, Activated carbons for the adsorption of ibuprofen, Carbon 45 (2007) 1979–1988.